

## Drawing 3-Polytopes with Good Vertex Resolution

*André Schulz*

Institut für Mathematische Logik und Grundlagenforschung,  
Universität Münster

### Abstract

We study the problem how to obtain a small drawing of a 3-polytope with Euclidean distance between any two points at least 1. The problem can be reduced to a one-dimensional problem, since it is sufficient to guarantee distinct integer  $x$ -coordinates. We develop an algorithm that yields an embedding with the desired property such that the polytope is contained inside a  $2(n-2) \times 2 \times 1$  box. The constructed embedding can be scaled to a grid embedding whose  $x$ -coordinates are contained in  $[0, 2(n-2)]$ . Furthermore, the point set of the embedding has a small spread, which differs from the best possible spread only by a multiplicative constant.

Submitted: December 2009	Reviewed: September 2010	Revised: October 2010	Accepted: November 2010
	Final: November 2010	Published: February 2011	
Communicated by: D. Eppstein and E. R. Gansner		Article type: Regular paper	

## 1 Introduction

Let  $G$  be a 3-connected planar graph with  $n$  vertices  $v_1, \dots, v_n$  and edge set  $E$ . A 3-polytope is a polytope in 3d with full dimension. The face lattice of a 3-polytope is entirely determined by its edge graph. Due to Steinitz' seminal theorem [19] we know that  $G$  admits a realization as the edge graph of a 3-polytope, and every edge graph of a 3-polytope is planar and 3-connected. The question arises how one can obtain a “nice” realization of a 3-polytope when its graph is given. One particular property, which is often desired from an aesthetically point of view, is that the vertices of the embedding should be evenly distributed. If two vertices lie too close together they are hard to distinguish. Such an embedding may appear as bad “illustration” for the human eye. Of course we can always scale a 3-polytope to increase all of its pointwise distances, but this does not affect the relative distances and the subjective perception of the viewer stays the same. Therefore, we restrict ourselves to an embedding whose vertices have, pairwise, an Euclidean distance of at least 1. We say that in this case the embedding/drawing is under the *vertex resolution rule*. See [2] for a short discussion on resolution rules. Resolution rules depend on a particular distance measure. Throughout the paper we use the Euclidean distance, but our results can be easily modified for other distance measures such as  $L_1$  or  $L_\infty$ .

In 2d, drawings of planar graphs can be realized on an  $O(n) \times O(n)$  grid [6, 16]. Since the grid is small, these grid embeddings give a good vertex resolution for free. The situation for 3-polytopes is different. The best known algorithm uses a grid of size  $O(2^{7 \cdot 21n})$  [1, 14]. Thus, the induced resolution might be bad for this embedding.

Let us briefly discuss some approaches for realizing  $G$  as 3-polytope. Steinitz' original proof is based on a transformation of  $G$  to the graph of the tetrahedron. The transformation consists of a sequence of local modifications that preserve the realizability of  $G$  as 3-polytope. The Koebe-Andreev-Thurston Theorem on circle packings gives another proof of Steinitz' Theorem (see for example Schramm [17]). This approach relies on non-linear methods which makes many geometric features of the constructed 3-polytope intractable. A third approach uses liftings of planar graphs with equilibrium stress (known as the Maxwell-Cremona correspondence [22]). In order to construct a plane embedding with equilibrium stress the intermediate 2d drawing is obtained as barycentric embedding by the method of Tutte [20, 21]. This powerful approach is used in a series of embedding algorithms: Eades and Garvan [7], Richter-Gebert [15], Chrobak, Goodrich, and Tamassia [2], Ribó Mor, Rote, and Schulz [14]. We refer to this approach as *lifting approach*. A completely different approach is due to Das and Goodrich [5]. It uses an incremental technique which only needs  $O(n)$  arithmetic operations for embedding  $G$  as 3-polytope, but works only for triangulated planar graphs.

**Outline:** We present an embedding algorithm that follows the popular lifting approach. Before presenting the algorithm in Section 5 we develop some necessary tools. In Section 2 we review the lifting approach. In particular, we

show how to compute a barycentric embedding and how to apply the Maxwell–Cremona correspondence. This part contains well-known concepts. In general it is not possible to lift a barycentric embedding. The applicability of the Maxwell–Cremona correspondence depends on the selected boundary. Thus we have to select the location of the boundary such that the 2d drawing is liftable. This can be achieved by the methods presented in [14]. For completeness we discuss this part in Section 3. Since we are interested in a 2d embedding that will give a good vertex resolution in the lifting we have to find a way to control the 2d embedding (presented in Section 4). This will be done by adjusting the barycentric weights that specify the 2d drawing. It suffices to guarantee small distinct integer  $x$ -coordinates to assure the vertex resolution rule. We follow the construction of [2] to guarantee distinct  $x$ -coordinates. In order to find an appropriate location of the boundary face we have to find a way to *control* the barycentric weights even further. These tools are crucial for the design of the algorithm and are developed in Section 4. After presenting the embedding algorithm in Section 5 we present additional properties of the computed embeddings in Section 6 and conclude with an example in Section 7.

**Results:** We show how to obtain an embedding of  $G$  as 3-polytope inside a  $2(n-2) \times 2 \times 1$  box under the vertex resolution rule. It is even possible to make the box arbitrarily flat such that its volume gets arbitrarily small. But for aesthetic reasons we leave the side lengths at least 1. Our algorithm follows the lifting approach and extends the ideas of [14]. In contrast to the construction of [14] we use more complicated interior edge weights. Our algorithm creates an embedding with two more interesting properties: (1) it can be scaled to a grid embedding whose  $x$ -coordinates are in  $[0, 2(n-2)]$ , and (2) the point set of the embedding has a good ratio between its largest and shortest pointwise distance. We show that this number differs only by a constant from the best possible ratio.

**Related work:** In [2] Chrobak, Goodrich, and Tamassia introduced an algorithm that embeds a 3-polytope inside an  $O(n) \times O(1) \times O(1)$  box under the vertex resolution rule. However, this result was only published as preliminary version, without giving all details. For example, it was not mentioned how to derive the prescribed set of  $x$ -coordinates. More severely, the algorithm is only applicable for polytopes that contain a triangular face. We reuse some of the ideas of [2], but especially the more complicated case where the polytope does not have a triangular face requires completely new techniques. In order to follow the lifting approach for polytopes that do not contain a triangular face, we apply the techniques of [14]. By relabeling the vertices of the outer face it is possible to make quantitative assumptions of the induced barycentric weights on the boundary face. This idea finds application in [14] and was used to find an appropriate location of the boundary face. This argument is not applicable in our setting, because we want to maintain fixed  $x$ -coordinates and cannot shift the vertex labels. In order to control the induced weights on the boundary we

have to make use of the new techniques developed in Lemma 4 and 5.

## 2 Preliminaries: Maxwell and Tutte

In this section we review Tutte's barycentric 2d embeddings and the Maxwell-Cremona correspondence. Both tools are well established necessary ingredients for the lifting approach.

Since  $G$  is 3-connected and planar, the facial structure of  $G$  is uniquely determined [23]. Let us pick an arbitrary face  $f_b$ , which we call the *boundary face*. We assume further that the vertices are ordered such that  $v_1, v_2, \dots, v_k$  are the vertices of  $f_b$  in cyclic order. An edge (vertex) is called a *boundary edge (vertex)* if it lies on  $f_b$ , otherwise it is called an *interior edge (vertex)*. In this paper every embedding is considered as plane straight-line embedding. A 2d embedding of  $G$  is specified by giving every vertex  $v_i$  a coordinate  $\mathbf{p}_i = (x_i, y_i)^T$ . We denote the 2d embedding as  $G(\mathbf{p})$  and consider only embeddings that realize  $f_b$  as a convex outer face.

To describe the Maxwell-Cremona correspondence we introduce the concept of *equilibrium stresses*.

**Definition 1 (Stress, Equilibrium)** *An assignment  $\omega: E \rightarrow \mathbb{R}$  of scalars to the edges of  $G$  (with  $\omega(i, j) =: \omega_{ij} = \omega_{ji}$ ) is called a stress. Let  $G(\mathbf{p})$  be a 2d embedding of  $G$ . A point  $\mathbf{p}_i$  is in equilibrium if and only if*

$$\sum_{j:(i,j) \in E} \omega_{ij}(\mathbf{p}_i - \mathbf{p}_j) = \mathbf{0}. \quad (1)$$

*The embedding of  $G$  is in equilibrium if and only if all of its points are in equilibrium.*

If  $G(\mathbf{p})$  is in equilibrium according to  $\omega$ , then  $\omega$  is called an *equilibrium stress* for  $G(\mathbf{p})$ . Of special interest are stresses that are positive on every interior edge of  $G$ . These stresses are called *positive stresses*.

Suppose we fix an embedding  $G(\mathbf{p})$  in the plane. Let  $h: V \rightarrow \mathbb{R}$  be a height assignment for the vertices of  $G$ . The function  $h$  defines a 3d embedding of  $G$  by giving every vertex  $\mathbf{p}_i$  the additional  $z$ -coordinate  $z_i = h(\mathbf{p}_i)$ . If in the 3d embedding every face of  $G$  lies on a plane the height assignment  $h$  is called a *lifting*. The Maxwell-Cremona correspondence describes the following.

**Theorem 1 (Maxwell [12], Whiteley [22])** *Let  $G$  be a 3-connected planar graph with 2d embedding  $G(\mathbf{p})$  and a designated face  $\hat{f}$ . There exists an 1-1 correspondence between*

- A.) *equilibrium stresses  $\omega$  on  $G(\mathbf{p})$ ,*
- B.) *liftings of  $G(\mathbf{p})$  in  $\mathbb{R}^3$ , where face  $\hat{f}$  lies in the  $xy$ -plane.*

*If the stress is positive, the lifting yields a convex 3-polytope.*

The complete proof of the Maxwell-Cremona correspondence is due to Whiteley [22] (see also [4]). Richter-Gebert’s book [15, Section 13] contains a simple algorithm that computes the lifting: The location of every face in the lifting is specified by  $G(\mathbf{p})$  and a plane on which the face lies. For convenience we introduce for every vertex  $\mathbf{p}_i = (x_i, y_i)^T$  a (homogenized) 3d vertex  $\mathbf{p}'_i := (x_i, y_i, 1)^T$ . We define for every face  $f_j$  a vector  $\mathbf{q}_j \in \mathbf{R}^3$ , such that  $\langle \mathbf{q}_j, \mathbf{p} \rangle$  describes the height of the point  $\mathbf{p} \in f_j$  in the lifting. The vectors  $\mathbf{q}_j$  can be computed incrementally by

$$\begin{aligned} \mathbf{q}_b &= (0, 0, 0)^T, \\ \mathbf{q}_l &= \omega_{ij}(\mathbf{p}'_i \times \mathbf{p}'_j) + \mathbf{q}_r, \end{aligned} \tag{2}$$

where the edge pointing from  $i$  to  $j$  separates the faces  $f_l$  and  $f_r$ , such that  $f_l$  lies to the left and  $f_r$  lies to the right. Notice that the computed lifting does not depend on the order of the faces that is used to determine the  $\mathbf{q}$  vectors.

To apply the Maxwell-Cremona correspondence one needs a 2d embedding of  $G$  with equilibrium stress. Barycentric embeddings can generate drawings for which the equilibrium condition (1) holds for all interior vertices. Let  $\omega$  be an arbitrary stress that is positive on the interior edges and zero on the boundary edges. (It is valid to select stresses of value 0 on the boundary because the boundary stress weights do not affect the barycentric embedding.) We obtain from the stress  $\omega$  its *Laplace matrix*  $L = \{l_{ij}\}$ , which is defined by its entries as

$$l_{ij} := \begin{cases} -\omega_{ij} & \text{if } (i, j) \in E \text{ and } i \neq j, \\ \sum_j \omega_{ij} & \text{if } i = j, \\ 0 & \text{otherwise.} \end{cases}$$

An embedding  $G(\mathbf{p})$  is described by the vectors  $\mathbf{x} = (x_1, \dots, x_n)^T$  and  $\mathbf{y} = (y_1, \dots, y_n)^T$ . Let  $B := \{1, \dots, k\}$  and  $I := \{k + 1, \dots, n\}$  be the index sets of the boundary and interior vertices, respectively. We subdivide  $\mathbf{x}, \mathbf{y}$ , and  $L$  by  $B$  and  $I$  and obtain  $\mathbf{x}_B, \mathbf{x}_I, \mathbf{y}_B, \mathbf{y}_I, L_{BB}, L_{II}, L_{BI}$  and  $L_{IB}$ . The equilibrium condition (1) for the interior vertices can be phrased as  $L_{IB}\mathbf{x}_B + L_{II}\mathbf{x}_I = \mathbf{0}$ . The same holds for the  $y$ -coordinates. This implies that we can express the vectors  $\mathbf{x}_I$  and  $\mathbf{y}_I$  as linear functions in terms of  $\mathbf{x}_B$  and  $\mathbf{y}_B$ , namely by

$$\mathbf{x}_I = -L_{II}^{-1}L_{IB}\mathbf{x}_B, \quad \mathbf{y}_I = -L_{II}^{-1}L_{IB}\mathbf{y}_B. \tag{3}$$

The matrix  $L_{II}$  is singular and hence the vectors  $\mathbf{x}_I$  and  $\mathbf{y}_I$  are properly and uniquely defined (see [15, 8]). The embedding is known as the (weighted) barycentric embedding. For every positive stress and convex boundary face the coordinates give a strictly convex straight-line embedding (see for example [8]). A weighted barycentric embedding has the following nice interpretation: The interior edges of the graph can be considered as springs with spring constants  $\omega_{ij}$ . The barycentric embedding models the equilibrium state of the system of springs when the boundary vertices are pinned at their fixed positions.

### 3 Extending an Equilibrium Stress to the Boundary

The interior vertices computed by (3) are in equilibrium by construction. However, the stressed edges of the boundary vertices do not sum up to zero, but to

$$\forall i \in B \quad \sum_{j:(i,j) \in E} \omega_{ij}(\mathbf{p}_i - \mathbf{p}_j) =: \mathbf{F}_i. \quad (4)$$

To apply the Maxwell-Cremona correspondence we have to alter the stress on the boundary edges (which we set to 0) such that it cancels the vectors  $\mathbf{F}_i$ . Adjusting the stress weights on the boundary does not interfere with the barycentric embedding. If the outer face is a triangle it is always possible to cancel the  $\mathbf{F}_i$  vectors by solving a linear system with three unknowns [9]. But in general this is only possible for special locations of the boundary face. We use the method of Ribó Mor, Rote, and Schulz [14] to extend the equilibrium stress to the boundary.

**Lemma 1 (Substitution Lemma [14])** *There are weights  $\tilde{\omega}_{ij} = \tilde{\omega}_{ji}$ , for  $i, j \in B$ , independent of location of the boundary face such that*

$$\forall i \in B \quad \mathbf{F}_i = \sum_{j \in B: j \neq i} \tilde{\omega}_{ij}(\mathbf{p}_i - \mathbf{p}_j). \quad (5)$$

*The weights  $\tilde{\omega}_{ij}$  are the off-diagonal entries of  $-L_{BB} + L_{BI}L_{II}^{-1}L_{IB}$ , which is the Schur Complement of  $L_{II}$  in  $L$  multiplied with  $-1$ .*

The proof of the Substitution Lemma can be found in [14]. The  $\tilde{\omega}$  values are independent of the location of the boundary face and depend only on the stress  $\omega$ . From this point of view we can use the complete graph  $K_k$  on the boundary vertices with stress  $\tilde{\omega}$  as substitution for the embedding  $G(\mathbf{p})$  with stress  $\omega$  to express the vectors  $\mathbf{F}_i$ . For this reason we call the stress  $\tilde{\omega}$  the *substitution stress*. The different weights  $\tilde{\omega}_{ij}$  are named *substitution stress entries*. With help of the substitution stress we can simplify the problem of locating the boundary face. A feasible location of  $f_b$  can be found by solving the non-linear system consisting of the  $2k$  equations of (5) ( $k$  equations for the  $x$ -coordinates, and  $k$  equations for the  $y$ -coordinates) plus the  $2k$  equations

$$\forall i \in B : \omega_{i,suc(i)}(\mathbf{p}_i - \mathbf{p}_{suc(i)}) + \omega_{i,pre(i)}(\mathbf{p}_i - \mathbf{p}_{pre(i)}) = -\mathbf{F}_i, \quad (6)$$

where  $suc(i)$  denotes the successor of  $v_i$  and  $pre(i)$  denotes the predecessor of  $v_i$  on  $f_b$  in cyclic order. Since the equations are dependent the system is under-constrained. Later, we will fix some boundary coordinates to obtain a unique solution. An important property of the substitution stress entries was observed in [14].

**Lemma 2 (Lemma 3.3(1) in [14])** *If the stress  $\omega$  is positive, then for every  $i, j \in B$  the induced substitution stress  $\tilde{\omega}_{ij}$  is positive.*

The proof of the lemma can be found in [14].

## 4 Constructing and Controlling an $x$ -Equilibrium Stress

So far we followed the ideas of [14] and showed how to construct an embedding with equilibrium stress by using a barycentric embedding whose position of the outer face was computed in advance by a non-linear system. In order to use a barycentric embedding properly one has to show that the pre-computed outer face forms a convex polygon. This is only possible by deriving structural properties for the substitution stress. In addition to the construction of [14] we have to show that the vertex resolution rule holds. We explain in this section how to modify the barycentric weights, such that a set of prescribed  $x$ -coordinates are the solution of the barycentric embedding. Moreover we show how to update the barycentric weights further, such that one or two substitution stress entries become dominant while preserving the  $x$ -coordinates. Our goal is to select small distinct integer values for the  $x$ -coordinates, which would imply the vertex resolution rule. The structural property of the dominating stress entries will be later useful if we have to show that the boundary face is realized as convex polygon.

Let  $x_1, \dots, x_n$  now be the prescribed  $x$ -coordinates we want to achieve in  $G(\mathbf{p})$ . We are interested in a positive equilibrium stress that yields these  $x$ -coordinates in the barycentric embedding. In particular, we are looking for a positive stress  $\omega$  such that

$$\forall i \in I \quad \sum_{j:(i,j) \in E} \omega_{ij}(x_i - x_j) = 0. \quad (7)$$

We call a positive stress that fulfills condition (7) a (positive)  $x$ -equilibrium stress. Since we consider in this paper only positive  $x$ -equilibrium stresses we omit the term “positive” in the following. A simple directed path  $\pi = v_{i_1}, v_{i_2}, \dots$  in  $G$  is called  $x$ -monotone if for all its vertices  $v_{i_k}$  we have  $x_{i_k} < x_{i_{k+1}}$ . As pointed out in [2], an  $x$ -equilibrium stress exists if every interior edge lies on some  $x$ -monotone path, whose endpoints are boundary vertices. Let us assume that we have selected the  $x$ -coordinates such that the latter holds. Furthermore, let us pick for every edge  $e$  some  $x$ -monotone path  $P_e$ .

We follow the approach of [2] to construct an  $x$ -equilibrium stress. The construction is based on assigning a cost  $c_{\{i,j\}} > 0$  to every interior edge  $(i, j)$  of  $G$ . If the costs guarantee

$$\forall i \in I \quad \sum_{j:(i,j) \in E: x_i < x_j} c_{\{i,j\}} = \sum_{(i,k) \in E: x_i > x_k} c_{\{i,k\}}, \quad (8)$$

we can define an  $x$ -equilibrium stress by setting

$$\omega_{ij} = \frac{c_{\{i,j\}}}{|x_i - x_j|}. \quad (9)$$

The costs  $c_{\{i,j\}}$  can be constructed by the following incremental construction. We start with  $c_{\{i,j\}} \equiv 0$  and increase the costs successively. Let  $e = (i, j)$  be

an edge with  $c_{\{i,j\}} = 0$ . We increase the costs of the edges of  $P_e$  by 1. In (8) both sides of the equation increase by 1 if  $v_i$  lies on  $P_e$ , otherwise nothing changes. Hence, (8) still holds. We repeat this procedure until every interior edge is assigned with a positive cost. Since we have at most  $3n - 3$  interior edges, the total cost for an edge is an integer smaller than  $3n - 3$ .

We show now how to modify an  $x$ -equilibrium stress to obtain helpful properties for the substitution stress induced by  $\omega$ . Our goal is to obtain a substitution stress that realizes its maximal entry on an edge that we picked. More formally, let  $v_s$  and  $v_t$  be two non-adjacent vertices on the boundary of  $G$  and let  $\alpha > 1$  be a parameter that we pick later. The stress  $\omega$  should guarantee that for all pairs of boundary vertices  $v_i, v_j$  we have  $\tilde{\omega}_{st} > \alpha \tilde{\omega}_{ij}$ , unless  $\{i, j\} = \{s, t\}$ . Our idea for how to achieve this is the following: We pick an  $x$ -monotone path  $P_{st}$  from  $v_s$  to  $v_t$ . Then we determine a suitable (large) number  $K$ , and add  $K$  to the costs of every edge which is on  $P_{st}$ . The stress induced by the increased costs is still an  $x$ -equilibrium stress for our choice of  $x$ -coordinates. If we think of the stresses as spring constants, we have increased the force that pushes  $v_s$  and  $v_t$  away from each other. Our hope is that this will reflect in the substitution stress and make  $\tilde{\omega}_{st}$  the dominant stress entry.

First, let us bound the substitution stress on all edges from above and then prove a lower bound for the stress  $\tilde{\omega}_{st}$ .

**Lemma 3** *Let  $L = \{l_{ij}\}$  be the Laplace matrix derived from a positive stress  $\omega$ , and  $\tilde{\omega}$  the corresponding substitution stress. For any  $i, j \in B$  we have*

$$\tilde{\omega}_{ij} < \min\{l_{ii}, l_{jj}\}.$$

**Proof:** Since  $\mathbf{u}^T L \mathbf{u} = \sum_{(i,j) \in E} \omega_{ij} (u_i - u_j)^2$ , which is non-negative for any vector  $\mathbf{u}$ , the Laplace matrix is positive semidefinite. Let  $\tilde{L} = \{\tilde{l}_{ij}\} = L_{BB} - L_{BI} L_{II}^{-1} L_{IB}$  denote the Schur complement of  $L_{II}$  in  $L$ . Due to [24, page 175]  $L_{II} - \tilde{L}$  is positive semidefinite. Therefore, all principal submatrices are positive semidefinite and we have  $l_{ii} \geq \tilde{l}_{ii}$ . As a consequence of the substitution lemma, we know that  $\sum_{j \in B: i \neq j} \tilde{\omega}_{ij} = \tilde{l}_{ii}$ , and hence  $\sum_{j \in B: i \neq j} \tilde{\omega}_{ij} \leq l_{ii}$ . Since each of the  $\tilde{\omega}_{ij}$ 's is positive, each summand has to be smaller than  $l_{ii}$ . By the same argument  $\tilde{\omega}_{ij} \leq l_{jj}$ , which proves the lemma.  $\square$

The next lemma proves a lower bound for  $\tilde{\omega}_{st}$  and determines the number  $K$  that guarantees that  $\tilde{\omega}_{st}$  becomes the dominant stress.

**Lemma 4** *Let  $\omega$  be an  $x$ -equilibrium stress obtained from the edge costs  $c_{\{i,j\}} < 3n$  for  $x_1, \dots, x_n$  that is increased along an  $x$ -monotone path from  $v_s$  to  $v_t$ , by incrementing the edge costs for edges on the path by  $K$ . The substitution stress and the matrix  $L$  are obtained from  $\omega$  as usual. Then*

$$\tilde{\omega}_{st} > \frac{K - 3n^2(1 + (k - 2)\Delta_x)}{x_t - x_s},$$

where  $k$  denotes the number of boundary vertices and  $\Delta_x$  the largest distance between two  $x$ -coordinates. For any  $\alpha > 0$  we can pick  $K \geq 3n^2(1 + (\alpha + k - 2)\Delta_x)$

and obtain for any  $\tilde{\omega}_{ij}$  that is not  $\tilde{\omega}_{st}$

$$\tilde{\omega}_{st} > \alpha \tilde{\omega}_{ij}.$$

**Proof:** Before bounding  $\tilde{\omega}_{st}$  we show an upper bound for the other substitution stress entries. Let  $(i, j)$  an edge that is not  $(s, t)$ . By Lemma 3,  $\tilde{\omega}_{ij}$  is less than  $l_{rr}$  ( $r \in \{i, j\} \setminus \{s, t\}$ ). Since  $l_{rr}$  is a diagonal entry of the Laplace matrix it equals  $\sum_{u:(r,u) \in E} \omega_{ru}$ , which is a sum of at most  $n - 1$  summands. We can assume that the path  $P_{st}$  uses no boundary edge. In this case each summand in  $\sum_{u:(r,u) \in E} \omega_{ru}$  is smaller than  $3n$  and we obtain

$$\forall \{i, j\} \neq \{s, t\} \quad \tilde{\omega}_{ij} < \max_{r \in B \setminus \{s, t\}} \{l_{rr}\} < 3n^2. \quad (10)$$

Let  $F_t^x$  be the  $x$ -component of  $\mathbf{F}_t$ . We combine (10) and (5) and obtain as upper bound for  $F_t^x$

$$\tilde{\omega}_{st}(x_t - x_s) + (k - 2)3n^2\Delta_x > F_t^x.$$

On the other hand we can express  $F_t^x$  by (4). The cost of one edge  $(w, t)$ , with  $x_w < x_t$ , was increased by  $K$ . All other costs are in total less than  $3n^2$ . Thus,

$$F_t^x = \sum_{u:(u,t) \in E} \omega_{ut}(x_t - x_u) = \sum_{\substack{u:x_u < x_t \\ (u,t) \in E}} c_{\{t,u\}} - \sum_{\substack{v:x_v > x_t \\ (v,t) \in E}} c_{\{t,v\}} > K - 3n^2.$$

Combining the two bounds for  $F_t^x$  leads to the bound for  $\tilde{\omega}_{st}$  as stated in the lemma. Setting  $K \geq 3n^2(1 + (\alpha + k - 2)\Delta_x)$  yields

$$\tilde{\omega}_{st} > \frac{3n^2(\alpha + k - 2)\Delta_x - 3n^2(k - 2)\Delta_x}{x_t - x_s} = \frac{3n^2\alpha\Delta_x}{x_t - x_s} \geq 3n^2\alpha > \alpha\tilde{\omega}_{ij}.$$

□

As the last part of this section we show that we can even enforce a pair of substitution stress entries to be dominant if we have at least 5 vertices on the boundary face. Let  $v_{t_1}, v_{t_2}$  be two vertices that are both non-adjacent to  $v_s$  and let  $x_{t_1} = x_{t_2}$ . We can increment a given  $x$ -equilibrium stress by first increasing the edge costs  $c_{\{i,j\}}$  along an  $x$ -monotone path from  $v_s$  to  $v_{t_1}$  by  $K$  and then do the same for an appropriate path from  $v_s$  to  $v_{t_2}$ .

**Lemma 5** *Assume the same as in Lemma 4, but this time consider two paths: from  $v_s$  to  $v_{t_1}$  and from  $v_s$  to  $v_{t_2}$ . Assume further that  $x_{t_1} = x_{t_2}$ . For  $K \geq 3n^2(1 + (\alpha + k - 2)\Delta_x)$  we have for any  $\tilde{\omega}_{ij}$  with  $\{i, j\} \not\subset \{s, t_1, t_2\}$*

$$\tilde{\omega}_{st_1} > \alpha\tilde{\omega}_{ij}, \text{ and } \tilde{\omega}_{st_2} > \alpha\tilde{\omega}_{ij}.$$

**Proof:** Lemma 4 relies on the fact that we can bound  $\sum_{j \neq s} \tilde{\omega}_{jt}(x_t - x_j)$  because by (10) the  $\tilde{\omega}$ 's in this sum are small. We cannot use this bound for  $\tilde{\omega}_{t_1 t_2}(x_{t_1} - x_{t_2})$  anymore, but this summand is irrelevant, since  $x_{t_1} = x_{t_2}$ . Following the

steps of the proof of Lemma 4 with first choosing  $t = t_1$  and then choosing  $t = t_2$  proves the lemma.  $\square$

Notice that the bounds for  $K$  are very rough. Better bounds can be easily obtained, but they result in more complicated expressions. Since for our purpose the fact that we can always find a valid number  $K$  is more important than the smallest possible size of  $K$ , we presented a simple bound for  $K$ .

## 5 The Embedding Algorithm

### 5.1 The Algorithm Template

In this section we present as the main result of this paper

**Theorem 2** *Let  $G$  be a 3-connected planar graph.  $G$  admits an embedding as 3-polytope inside a  $2(n - 2) \times 2 \times 1$  box under the vertex resolution rule.*

We prove Theorem 2 in the remainder of this section by introducing an algorithm that constructs the desired embedding. The number of vertices on the boundary face plays an important role. The smaller this number is, the simpler is it to construct an embedding. For this reason we choose as boundary face  $f_b$  the smallest face of  $G$ . Due to Euler's formula  $f_b$  has at most 5 vertices. Depending on the size of  $f_b$  we obtain three versions of the algorithm which all follow the same basic pattern.

Our goal is to construct a planar embedding of  $G$  that has a positive stress and whose  $x$ -coordinates are distinct integers. The corresponding lifting of such an embedding fulfills the vertex resolution rule independently of its  $y$  and  $z$ -coordinates. Hence, we can scale in the direction of the  $y$  and  $z$ -axis without violating the vertex resolution rule. The basic procedure is summarized in Algorithm 1.

---

**Algorithm 1:** Embedding algorithm as template.

---

- 1: Choose the  $x$ -coordinates.
  - 2: Construct an  $x$ -equilibrium stress  $\omega$ .
  - 3: Choose the boundary  $y$ -coordinates.
  - 4: Embed  $G$  as barycentric embedding with stress  $\omega$  and the selected boundary in the plane.
  - 5: Lift the plane embedding.
- 

**Step 1:** The selection of the  $x$ -coordinates for  $G(\mathbf{p})$  is independent of the size of  $f_b$ . We start with some strictly convex plane embedding of  $G$  – called a *pre-embedding*. Let  $\hat{x}_1, \dots, \hat{x}_n$  and  $\hat{y}_1, \dots, \hat{y}_n$  be the coordinates of the pre-embedding which we compute as a barycentric embedding. In order to compute the barycentric embedding we have to fix the  $\hat{x}$ -coordinates of the boundary face.

The actual values of these coordinates depend on the size of  $f_b$ , and are given in Section 5.2–5.4. We assume that in the pre-embedding all  $x$ -coordinates are different. If this is not the case we can perturb the stress of the (pre)-embedding to achieve this. Since the pre-embedding is strictly convex [21] every edge lies on some  $x$ -monotone path. As it was done in Section 4, we fix for every interior edge  $e$  such a path  $P_e$ . The  $x$ -coordinates of the pre-embedding induce a strict linear order on the vertices of  $G$ . We denote with  $b_i$  the number of vertices with smaller  $\hat{x}$ -coordinate compared to  $\hat{x}_i$  in the pre-embedding. The  $x$ -coordinates of the (final) embedding are defined as  $x_i := b_i$ . Thus, no two vertices get the same  $x$ -coordinate and the largest  $x$ -coordinate is less than  $n$ . The paths  $P_e$  remain  $x$ -monotone in  $G(\mathbf{p})$ . Therefore, they can be used to define an appropriate  $x$ -equilibrium stress  $\omega$ . For technical reasons we might choose the same  $x$ -coordinate for some of the boundary vertices. In this case we check the vertex resolution rule for these vertex pairs in  $G(\mathbf{p})$  separately.

**Steps 2 and 3:** These steps are the difficult part of the algorithm. We have to choose the stress  $\omega$  and the boundary  $y$ -coordinates such that an extension of the stress to the boundary is possible. Moreover, the boundary coordinates have to yield a convex boundary face. After computing  $\omega$  we can derive the substitution stress. The feasible location of the boundary  $y$  coordinates is then expressed in terms of the substitution stress entries. We explain steps 2 and 3 in Section 5.2, 5.3 and 5.4 for the three different cases separately. To execute step 2 we have to apply the techniques developed in Section 3 and 4.

**Steps 4 and 5:** This part is a straightforward application of the barycentric embedding and the Maxwell-Cremona correspondence (see Section 2). The value of the (extended) stress on the boundary edges is not needed to compute the lifting, because we can place an interior face in the  $xy$ -plane and then compute the lifting using only interior edges.

## 5.2 Graphs with Triangular Face

The case where  $f_b$  is a triangle is the easiest case because we can extend every stress to the boundary for every location of the outer face (see Section 3). This case was already addressed by Chrobak, Goodrich and Tamassia [2]. The discussion in this section will prove the following statement:

**Proposition 1** *Let  $G$  be a 3-connected planar graph and let  $G$  contain a triangular face.  $G$  admits an embedding as 3-polytope inside an  $(n - 1) \times 1 \times 1$  box under the vertex resolution rule.*

**Proof:** Let us compute the pre-embedding with the boundary coordinates  $\hat{x}_1 = 0$ ,  $\hat{x}_2 = 1$ , and  $\hat{x}_3 = 0$ . We use the  $x$ -monotone paths  $P_e$  to compute a suitable  $x$ -equilibrium stress  $\omega$  as discussed in Section 4. Next we compute the barycentric embedding for  $\omega$  with boundary coordinates  $\mathbf{p}_1 = (0, 0)^T$ ,  $\mathbf{p}_2 = (n - 1, 0)^T$ , and  $\mathbf{p}_3 = (0, 1)^T$ . As result we obtain interior  $y$ -coordinates in the interval  $(0, 1)$ .

Any two vertices have distance at least 1, since their  $x$ -coordinates differ by at least 1. (This is not true for  $v_1$  and  $v_3$ , but their distance is  $y_3 - y_1 = 1$ .)  $\square$

### 5.3 Graphs with Quadrilateral Face

Let us now assume that  $G$  contains a quadrilateral but no triangular face. In this case it is not always possible to extend an equilibrium stress  $\omega$  to the boundary. The observations of Section 3 help us to overcome this difficulty.

**Proposition 2** *Let  $G$  be a 3-connected planar graph and let  $G$  contain a quadrilateral face.  $G$  admits an embedding as 3-polytope inside a  $2(n-2) \times 1 \times 1$  box under the vertex resolution rule.*

**Proof:** We use as boundary coordinates for the pre-embedding  $\hat{x}_1 = 0, \hat{x}_2 = 1, \hat{x}_3 = 1$ , and  $\hat{x}_4 = 0$ . The  $x$ -coordinates induced by the pre-embedding give  $x_2 = x_3 = n - 2$ . We redefine the boundary  $x$ -coordinates by setting  $x_3 = 2(n - 2)$ . This maintains the  $x$ -monotonicity of the paths  $P_e$ , but makes it easier to extend the stress to the boundary as we will see in the following.

Let  $\omega$  be the  $x$ -equilibrium stress for the selected  $x$ -coordinates. For the later analysis it is helpful to have a “dominant” substitution stress entry. We therefore modify  $\omega$  with the technique described in Section 4. After increasing the costs along an  $x$ -monotone path  $\pi$  from  $v_1$  to  $v_3$  by  $18n^3$  we can assume that  $\tilde{\omega}_{13} > \tilde{\omega}_{24}$ . This follows from the application of Lemma 4 with  $\alpha = 1$ ,  $\Delta_x = 2(n - 2)$ , and  $k = 4$ . For these values  $18n^3 > 3n^2(1 + (\alpha + k - 2)\Delta_x)$  and thus the increment of the costs along  $\pi$  suffices.

Let us now discuss how to extend the stress  $\omega$  to the boundary. To solve the non-linear system given by (5) and (6) we fix some of the boundary  $y$ -coordinates to obtain a unique solution. In particular, we set  $y_1 = 0, y_2 = 0$ , and  $y_4 = 1$ . As final coordinate we obtain<sup>1</sup>

$$y_3 = \frac{\tilde{\omega}_{24}}{2\tilde{\omega}_{13} - \tilde{\omega}_{24}}.$$

Since  $\tilde{\omega}_{13} > \tilde{\omega}_{24}$ , we can deduce that  $0 < y_3 < 1$ . Hence, all  $y$ -coordinates are contained in  $[0, 1]$ . Furthermore, we know that the only two vertices with the same  $x$ -coordinate, namely  $v_1$  and  $v_4$ , have the distance  $y_4 - y_1 = 1$ . Therefore the vertex resolution rule holds. Finally, we scale the induced lifting such that the largest  $z$ -coordinate equals 1.  $\square$

### 5.4 The general case

**Proof of Theorem 2.** To prove the theorem we can assume that the boundary face contains 5 vertices. The other cases were already covered by Proposition 1 and 2. This however is the most complicated case. We follow the construction of the proof of Proposition 2 and compute a pre-embedding. We choose as the  $x$ -coordinates for the pre-embedding of the outer face  $\hat{x}_1 = 0, \hat{x}_2 = 1, \hat{x}_3 = 1, \hat{x}_4 =$

<sup>1</sup>The solution of the non-linear system was obtained by computer algebra software.

0, and  $\hat{x}_5 = -\varepsilon$ , for  $\varepsilon > 0$  small enough to guarantee that all interior vertices get a positive  $\hat{x}$ -coordinate in the pre-embedding. The pre-embedding induces the desired  $x$ -coordinates for  $G(\mathbf{p})$  (step 1 of Algorithm 1). We change the induced  $x$ -coordinates on the boundary without changing the “monotonicity” of the paths  $P_e$  by setting  $x_1 = 0, x_2 = n - 2, x_3 = n - 2, x_4 = 0$ , and  $x_5 = -(n - 2)$ . For the later analysis it is helpful to have two “dominating” substitution stress entries. This can be achieved with the method introduced in Section 4: We increase the costs, that define  $\omega$  along an  $x$ -monotone path from  $v_5$  to  $v_2$ , and along an  $x$ -monotone path from  $v_5$  to  $v_3$ . The increment is in both cases  $36n^3$ . The application of Lemma 5 with  $\alpha = 3, k = 5$ , and  $\Delta_x = 2(n - 2)$  yields

$$\tilde{\omega}_{25} > 3\tilde{\omega}_{13}, \tilde{\omega}_{25} > 3\tilde{\omega}_{14}, \tilde{\omega}_{25} > 3\tilde{\omega}_{24}, \tilde{\omega}_{35} > 3\tilde{\omega}_{13}, \tilde{\omega}_{35} > 3\tilde{\omega}_{14}, \tilde{\omega}_{35} > 3\tilde{\omega}_{24}, \quad (11)$$

since  $36n^2 > 3n^2(1 + (\alpha + k - 2)\Delta_x)$ . We can apply the lemma, because  $x_2 = x_3$ .

Appropriate boundary  $y$ -coordinates can be obtained by solving the nonlinear system given by (5) and (6). As in the proof of Proposition 2 we fix some  $y$ -coordinates to obtain a unique solution. We set  $y_1 = -1, y_4 = 1$ , and  $y_5 = 0$ . This yields the two remaining  $y$ -coordinates

$$\begin{aligned} y_2 &= -2 - 2 \frac{\tilde{\omega}_{24}\tilde{\omega}_{13} - \tilde{\omega}_{13}^2 - \tilde{\omega}_{35}\tilde{\omega}_{14} - 2\tilde{\omega}_{13}\tilde{\omega}_{35}}{\tilde{\omega}_{24}\tilde{\omega}_{35} + \tilde{\omega}_{25}\tilde{\omega}_{13} + 2\tilde{\omega}_{25}\tilde{\omega}_{35}}, \\ y_3 &= 2 + 2 \frac{\tilde{\omega}_{24}\tilde{\omega}_{13} - \tilde{\omega}_{24}^2 - \tilde{\omega}_{14}\tilde{\omega}_{25} - 2\tilde{\omega}_{24}\tilde{\omega}_{25}}{\tilde{\omega}_{24}\tilde{\omega}_{35} + \tilde{\omega}_{25}\tilde{\omega}_{13} + 2\tilde{\omega}_{25}\tilde{\omega}_{35}}. \end{aligned}$$

Two things need to be checked for the solution for  $y_2$  and  $y_3$ : (1)  $f_b$  has to be convex and (2)  $y_3 - y_2$  has to be large enough to guarantee the vertex resolution rule. First we show that  $-2 < y_2$  and  $y_3 < 2$ , which would imply that  $f_b$  is convex if  $y_3 > y_2$ . The inequalities  $-2 < y_2$  and  $y_3 < 2$  hold, iff

$$\begin{aligned} \tilde{\omega}_{24}\tilde{\omega}_{13} - \tilde{\omega}_{13}^2 - \tilde{\omega}_{35}\tilde{\omega}_{14} - 2\tilde{\omega}_{35}\tilde{\omega}_{13} &< 0 \quad \text{and} \\ \tilde{\omega}_{24}\tilde{\omega}_{13} - \tilde{\omega}_{24}^2 - \tilde{\omega}_{14}\tilde{\omega}_{25} - 2\tilde{\omega}_{25}\tilde{\omega}_{24} &< 0. \end{aligned}$$

Both inequalities are true, because as a consequence of (11) the only positive summand  $\tilde{\omega}_{24}\tilde{\omega}_{13}$  is smaller than  $\tilde{\omega}_{35}\tilde{\omega}_{13}$  and smaller than  $\tilde{\omega}_{25}\tilde{\omega}_{24}$ . The difference  $y_3 - y_2$  equals

$$4 + 2 \frac{2\tilde{\omega}_{24}\tilde{\omega}_{13} - \tilde{\omega}_{13}^2 - \tilde{\omega}_{24}^2 - \tilde{\omega}_{35}(\tilde{\omega}_{14} + 2\tilde{\omega}_{13}) - \tilde{\omega}_{25}(\tilde{\omega}_{14} + 2\tilde{\omega}_{24})}{\tilde{\omega}_{24}\tilde{\omega}_{35} + \tilde{\omega}_{25}\tilde{\omega}_{13} + 2\tilde{\omega}_{25}\tilde{\omega}_{35}}.$$

Due to (11) we know that  $\tilde{\omega}_{14} + 2\tilde{\omega}_{24} < \tilde{\omega}_{35}$  and  $\tilde{\omega}_{14} + 2\tilde{\omega}_{13} < \tilde{\omega}_{25}$ . Thus

$$y_3 - y_2 > 4 + 2 \frac{2\tilde{\omega}_{24}\tilde{\omega}_{13} - \tilde{\omega}_{13}^2 - \tilde{\omega}_{24}^2 - 2\tilde{\omega}_{35}\tilde{\omega}_{25}}{\tilde{\omega}_{24}\tilde{\omega}_{35} + \tilde{\omega}_{25}\tilde{\omega}_{13} + 2\tilde{\omega}_{25}\tilde{\omega}_{35}} > 2.$$

The estimation holds since (again due to (11))  $\tilde{\omega}_{24}\tilde{\omega}_{35} > \tilde{\omega}_{24}^2$  and  $\tilde{\omega}_{25}\tilde{\omega}_{13} > \tilde{\omega}_{13}^2$ , and hence the fraction is greater  $-1$ .

We multiply all  $y$ -coordinates with  $1/2$ . This yields  $y_4 - y_1 = 1$  and  $y_3 - y_2 > 1$ . The  $z$ -coordinates are scaled such that they lie between 0 and 1. Clearly, the vertex resolution rule holds for the computed embedding.  $\square$

We finish this section with some remarks on the running time of the embedding algorithm. As mentioned in [2] the  $x$ -equilibrium stress can be computed in linear time. The barycentric embedding (which we use twice, once for the pre-embedding and once for the intermediate plane embedding) can be computed by the linear system (3). Since the linear system is based on a planar structure, it can be solved with nested dissections (see [10, 11]) based on the planar separator theorem. As a consequence a solution can be computed in  $O(M(\sqrt{n}))$  time, where  $M(n)$  is the upper bound for multiplying two  $n \times n$  matrices. The current record for  $M(n)$  is  $O(n^{2.325})$ , which is due to Coppersmith and Winograd [3]. The computation of the lifting can be done in linear time. In total, we achieve a running time of  $O(n^{1.1625})$ .

## 6 Additional Properties of the Embedding

### 6.1 Induced Grid Embedding

In addition to the small embedding under the vertex resolution rule, the constructed embedding has several other nice properties which we discuss in this section. Since the computed  $y$  and  $z$ -coordinates are expressed by a linear system of rational numbers, they are rational numbers as well. Thus, we can scale the final embedding to obtain a grid embedding. We first prove a technical lemma.

**Lemma 6** *Suppose that all  $x$  and  $y$ -coordinates as well as the stress  $\omega$  are integral. Let the difference between two  $x$ -coordinates be less than  $\Delta_x$  and let the difference between two  $y$ -coordinates be less than  $\Delta_y$ . Then the height  $z_i$  of any point  $\mathbf{p}_i$  in the lifting is an integer and it can be bounded by*

$$0 \leq z_i \leq |\omega_{12}| \cdot \Delta_x \cdot \Delta_y,$$

where  $\omega_{12}$  is a stress on an arbitrary boundary edge.

**Proof:** Since by (2) all heights can be expressed as additions and multiplications of integers, the heights are integral. Moreover, all heights are invariant under rigid motions of the plane embedding. Hence, we can assume that  $y_1 = y_2 = 0$ ,  $x_1 = 0$ , and all  $y$ -coordinates are non-negative. The lifted polytope lies between the planes that contain the faces incident to the edge  $(1, 2)$ . One of these faces is the face  $f_b$ , which lies in the plane  $z = 0$ . Let the other face be  $f_1$ . We denote by  $\mathbf{p}_{max}$  the vertex that attains the maximal height  $z_{max}$  in the lifting. For the homogenized vertex  $\mathbf{p}'_{max}$  we have  $\langle \mathbf{p}'_{max}, \mathbf{q}_1 \rangle \geq z_{max}$ . Due to (2)  $\mathbf{q}_1 = \omega_{12}(0, -x_2, 0)^T$ , and hence  $|\omega_{12}| \cdot \Delta_x \cdot \Delta_y \geq \langle \mathbf{p}'_{max}, \mathbf{q}_1 \rangle$  and the lemma follows.  $\square$

**Theorem 3** *The embedding computed with Algorithm 1 can be scaled to integer coordinates such that*

$$\begin{aligned} 0 &\leq x_i \leq 2(n-2), \\ 0 &\leq y_i, z_i \leq 2^{O(n^2 \log n)}. \end{aligned}$$

**Proof:** We begin with analyzing the case where the boundary face is a pentagon. We multiply the computed stress  $\omega$  with  $n!$  and obtain an integral stress  $\omega'$ . Let  $L'$  be the Laplace matrix induced by the scaled stress. The substitution stress  $\tilde{\omega}$  is defined by the off-diagonal entries of  $L'_{BI}L'_{II}^{-1}L'_{IB}$ . Since we have an integral stress  $\omega'$  the entries of  $L'$  are integral as well. Due to the adjoint formula for the inverse of a matrix, the substitution stress entries are rational numbers and multiples of  $1/\det L'_{II}$ .

The  $y$ -coordinates of the embedding are computed as  $\mathbf{y}_I = -L'_{II}^{-1}L'_{IB}\mathbf{y}_B$ . We multiply the vector  $\mathbf{y}_B$  with  $(\tilde{\omega}_{24}\tilde{\omega}_{35} + \tilde{\omega}_{25}\tilde{\omega}_{13} + 2\tilde{\omega}_{25}\tilde{\omega}_{35})(\det L'_{II})^2$  to make it integral. Scaling the stress leaves the barycentric embedding unchanged. Due to Cramer's rule and (3) we have for every interior vertex  $v_i$

$$y_i = \frac{\det L'_{II}(i)}{\det L'_{II}},$$

where  $L'_{II}(i)$  denotes the matrix  $L'_{II}$  with row  $i$  substituted by  $\mathbf{y}_B$ . Since  $\det L'_{II}(i)$  is integral the interior  $y$ -coordinates are multiples of  $1/\det L'_{II}$ . Thus multiplying  $\mathbf{y}_B$  (again) with  $\det L'_{II}$  gives integer  $y$ -coordinates. In total we scale by  $(\tilde{\omega}_{24}\tilde{\omega}_{35} + \tilde{\omega}_{25}\tilde{\omega}_{13} + 2\tilde{\omega}_{25}\tilde{\omega}_{35})(\det L'_{II})^3$ , which is clearly dominated by  $(\det L'_{II})^3$ . Let us now discuss how to bound  $\det L'_{II}$ . Since  $L'$  is positive semidefinite,  $L'_{II}$  as principal submatrix is positive semidefinite as well. Therefore, we can bound the determinant by Hadamard's inequality (see [24, page 176]) and obtain

$$\det L'_{II} \leq \prod_{i=6}^n l'_{ii}.$$

Each entry  $l'_{ii}$  equals  $\sum_{u:(i,u) \in E} \omega'_{iu}$ . Without scaling each  $\omega_{ij}$  is bounded by  $O(n^3)$ . Hence, every  $\omega'_{ij}$  is in  $O(n!)$  and so is  $l'_{ii}$ . This implies that  $(\det L'_{II})^3$  is bounded by  $2^{O(n^2 \log n)}$ .

Next we bound the  $z$ -coordinates with help of Lemma 6. Let us first discuss how to bound  $\omega_{12}$ . Remember that the  $x$ -equilibrium stress was constructed by assigning costs to  $x$ -monotone paths. Instead of considering  $x$ -monotone paths one can use cycles to define an appropriate stress. Such a cycle consists of the old  $x$ -monotone path and closes this path by a path over the boundary. The  $x$ -monotone increasing path of the cycle adds a  $+1$  to the total costs of its edges – the  $x$ -monotone decreasing path adds a  $-1$  to the costs of its edges. We have to route only one of the cycles via the edge  $(1, 2)$ . This implies that  $\omega'_{12} = -n!/|x_1 - x_2|$ . Applying Lemma 6 leads to the bound for the largest  $z$ -coordinate of  $O(n! \cdot 2n \cdot (\det L'_{II})^3) = 2^{O(n^2 \log n)}$ .

The other two cases ( $k = 3, 4$ ) require smaller coordinates on the grid. We can mimic the analysis for the pentagon case, but since the denominator of the boundary  $y$ -coordinates is smaller (or to be precise, its upper bound is smaller) the scaling factor for the  $y$ -coordinates is smaller.  $\square$

Compared to the grid embedding presented in [14], we were able to reduce the size of the  $x$ -coordinates (from  $2n \cdot 8.107^n$  to  $2(n - 2)$ ) at the expense of

the  $y$  and  $z$ -coordinates (the embedding in [14] uses no coordinates greater than  $2^{\mathcal{O}(n)}$ ).

## 6.2 Spread of the Embedding

The *spread* of a point set is the quotient of the longest pairwise distance (the diameter) and the shortest pairwise distance. The smaller this ratio is, the more densely packed is the point set. A small spread implies that the points are “evenly distributed”. We define as *spread of an embedding of a polytope* the spread of its points.

**Theorem 4** *The spread of a 3-polytope embedded by Algorithm 1 is smaller than  $2n$ . There are polytopes without an embedding with spread smaller than  $(n - 1)/\pi$ .*

**Proof:** Let us first analyze the spread of the constructed 3-polytope. The diameter of its point set depends on the size of the boundary face. In all three cases it is smaller than  $2n$ . Since the smallest distance is larger than 1 the spread is less than  $2n$ .

We discuss now how large the spread of a 3-polytope can be. We assume that the embedding is scaled such that the smallest pointwise distance equals 1. Let  $G$  be the graph of a 3-dimensional pyramid. In any realization as 3-polytope the perimeter of its  $(n - 1)$ -gonal base is larger than  $n - 1$ . Since for convex sets the perimeter is smaller  $\pi$  times the diameter [18], we have that the spread of the  $(n - 1)$ -gon (and hence the spread of the pyramid) is larger than  $(n - 1)/\pi$ .  $\square$

Notice that in the 2d setting the points of the intermediate plane embedding of  $G$  have also a spread smaller than  $n$ . By the arguments of the proof of Theorem 4, a convex drawing of an  $n$ -gon needs a point set of spread  $n/\pi$ . Thus, for convex 2d drawings, the intermediate plane embedding of our algorithm has a spread that differs from the best possible only by a constant multiplicative factor.

## 7 An Example

We show as example how to realize a dodecahedron using Algorithm 1. The graph  $G$  of the dodecahedron is particularly suitable for a good example, because every face of  $G$  is a pentagon. Thus we have to apply the more complicated part of the algorithm. Due to the symmetry of  $G$  it does not matter which face we select as the boundary face. We follow our convention and name the vertices such that  $v_1, \dots, v_5$  belong to  $f_b$  in cyclic order.

We start with a plane drawing (the pre-embedding) of  $G$  with strictly convex faces and no vertical edges. Figure 1 shows our choice. The pre-embedding induces an order of the vertices which we use to define the  $x$ -coordinates, namely

$$\mathbf{x} = (0, 18, 18, 0, -18, 6, 3, 12, 13, 11, 15, 4, 7, 17, 14, 16, 5, 9, 10, 8)^T.$$

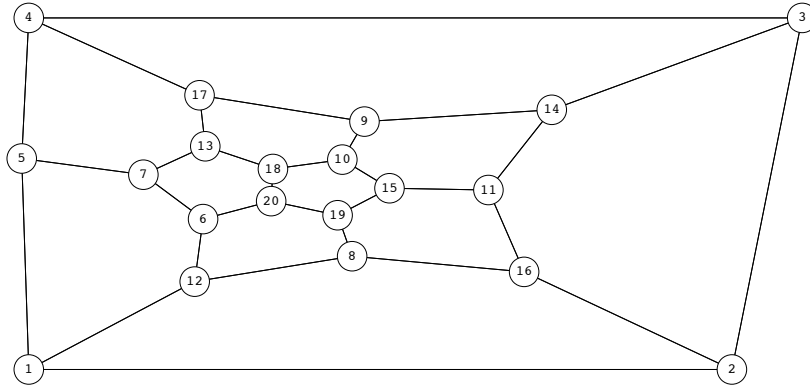


Figure 1: The pre-embedding of the dodecahedron.

The boundary  $x$ -coordinates are selected according to the algorithm. Next we construct the stress  $\omega$ . We select some  $x$ -monotone paths and compute the induced costs for the interior edges. The stress  $\omega$  induces the matrix  $\tilde{L}$ , which encodes the substitution stress by its off-diagonal entries (multiplied with -1). In our example we obtain

$$\tilde{L} = \begin{pmatrix} 0.234791 & -0.0769685 & -0.0815444 & -0.0354125 & -0.0408658 \\ -0.0769685 & 0.410969 & -0.264196 & -0.0401058 & \mathbf{-0.02969} \\ -0.0815444 & -0.264196 & 0.506504 & -0.108953 & \mathbf{-0.05181} \\ -0.0354125 & -0.0401058 & -0.108953 & 0.215884 & -0.031412 \\ -0.0408658 & \mathbf{-0.02969} & \mathbf{-0.05181} & -0.031412 & 0.153786 \end{pmatrix}.$$

It can be observed that the entries  $\tilde{l}_{35}$  and  $\tilde{l}_{25}$  are not the dominating entries. But for the correctness of the algorithm this is required. Indeed, for our current “choice” of the substitution stress, we would obtain the embedding shown in Figure 2(a). The figure illustrates that the too small substitution stress entries  $\tilde{\omega}_{25}$  and  $\tilde{\omega}_{35}$  cause a non-convex boundary face  $f_b$ . Fortunately, we can fix the problem by picking two  $x$ -monotone paths  $P_{25}$  and  $P_{35}$  and incrementing the costs on its edges by  $K$  (step 2 of the algorithm). We choose  $K$  according to Lemma 5. Since in our case  $n = 20$ ,  $\Delta x = 36$ ,  $\alpha = 3$ , and  $k = 5$ , it suffices to set  $K = 260\,400$ . The modified stress  $\omega$  gives now

$$\tilde{L} = \begin{pmatrix} 0.319465 & -0.151322 & -0.0666023 & -0.00126453 & -0.100277 \\ -0.151322 & 7.1641 & -2.97443 & -0.0515457 & \mathbf{-3.9868} \\ -0.066602 & -2.97443 & 7.22698 & -0.144387 & \mathbf{-4.04156} \\ -0.001264 & -0.0515457 & -0.144387 & 0.275482 & -0.0782853 \\ -0.100277 & \mathbf{-3.9868} & \mathbf{-4.04156} & -0.0782853 & 8.20693 \end{pmatrix}.$$

We observe that both  $\tilde{\omega}_{35}$  and  $\tilde{\omega}_{25}$  are greater than  $3\tilde{\omega}_{14}$ ,  $3\tilde{\omega}_{24}$  and  $3\tilde{\omega}_{13}$ . Therefore, we can continue with the algorithm and choose  $\mathbf{y}_B$  as described in Section 5.4. The induced barycentric embedding is shown in Figure 2(b) and the

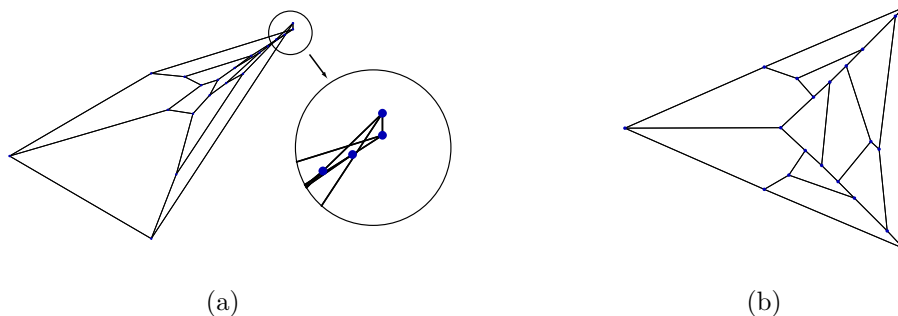


Figure 2: Embedding without (a) and with (b) making  $\tilde{\omega}_{25}$  and  $\tilde{\omega}_{35}$  dominant.

corresponding lifting is depicted in Figure 3(a). We did not execute the final scaling to obtain a more illustrative picture. Every face in the picture is drawn as strictly convex polygon. However, since we chose such a high value for  $K$  some edges become almost collinear. A more “spherical” embedding can be obtained by lowering the value for  $K$  and check whether this leaves  $y_3 - y_2 > 1$ . Such a drawing (for  $K = 10$ ) is shown in Figure 3(b).

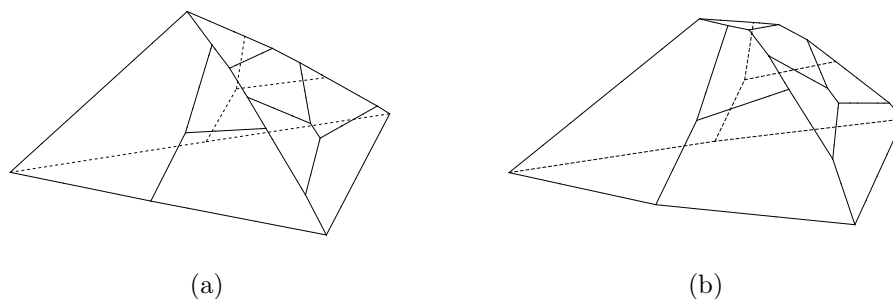


Figure 3: The final embedding (a) and the induced embedding for  $K = 10$  (b).

## Acknowledgments

I thank the anonymous reviewers, whose comments helped to improve the presentation of my results.

## References

- [1] K. Buchin and A. Schulz. On the number of spanning trees a planar graph can have. In M. de Berg and U. Meyer, editors, *ESA (1)*, volume 6346 of *Lecture Notes in Computer Science*, pages 110–121. Springer, 2010.
- [2] M. Chrobak, M. T. Goodrich, and R. Tamassia. Convex drawings of graphs in two and three dimensions (preliminary version). In *12th Symposium on Computational Geometry*, pages 319–328, 1996.
- [3] D. Coppersmith and S. Winograd. Matrix multiplication via arithmetic progressions. *J. Symb. Comput.*, 9(3):251–280, 1990.
- [4] H. Crapo and W. Whiteley. Plane self stresses and projected polyhedra I: The basic pattern. *Structural Topology*, 20:55–78, 1993.
- [5] G. Das and M. T. Goodrich. On the complexity of optimization problems for 3-dimensional convex polyhedra and decision trees. *Comput. Geom. Theory Appl.*, 8(3):123–137, 1997.
- [6] H. de Fraysseix, J. Pach, and R. Pollack. How to draw a planar graph on a grid. *Combinatorica*, 10(1):41–51, 1990.
- [7] P. Eades and P. Garvan. Drawing stressed planar graphs in three dimensions. In F.-J. Brandenburg, editor, *Graph Drawing*, volume 1027 of *Lecture Notes in Computer Science*, pages 212–223. Springer, 1995.
- [8] S. J. Gortler, C. Gotsman, and D. Thurston. Discrete one-forms on meshes and applications to 3d mesh parameterization. *Computer Aided Geometric Design*, 23(2):83–112, 2006.
- [9] J. E. Hopcroft and P. J. Kahn. A paradigm for robust geometric algorithms. *Algorithmica*, 7(4):339–380, 1992.
- [10] R. J. Lipton, D. Rose, and R. Tarjan. Generalized nested dissection. *SIAM J. Numer. Anal.*, 16(2):346–358, 1979.
- [11] R. J. Lipton and R. E. Tarjan. Applications of a planar separator theorem. *SIAM J. Comput.*, 9(3):615–627, 1980.
- [12] J. C. Maxwell. On reciprocal figures and diagrams of forces. *Phil. Mag. Ser.*, 27:250–261, 1864.
- [13] A. Ribó Mor, G. Rote, and A. Schulz. Embedding 3-polytopes on a small grid. In *SCG’07: Proc. 23rd Annual Symposium on Computational Geometry*, pages 112–118, New York, NY, USA, 2007. ACM.
- [14] A. Ribó Mor, G. Rote, and A. Schulz. Small grid embeddings of 3-polytopes. *Discrete Computational Geometry*, 2010. accepted for publication, preprint at <http://arxiv.org/abs/0908.0488>.

- [15] J. Richter-Gebert. *Realization Spaces of Polytopes*, volume 1643 of *Lecture Notes in Mathematics*. Springer, 1996.
- [16] W. Schnyder. Embedding planar graphs on the grid. In *Proc. 1st ACM-SIAM Sympos. Discrete Algorithms*, pages 138–148, 1990.
- [17] O. Schramm. Existence and uniqueness of packings with specified combinatorics. *Israel J. Math.*, 73:321–341, 1991.
- [18] P. R. Scott and P. W. Awyong. Inequalities for convex sets. *J. Ineq. Pure and Appl. Math.*, 1(1), 2000.
- [19] E. Steinitz. Encyclopädie der mathematischen Wissenschaften. In *Polyeder und Raumteilungen*, pages 1–139. 1922.
- [20] W. T. Tutte. Convex representations of graphs. *Proceedings London Mathematical Society*, 10(38):304–320, 1960.
- [21] W. T. Tutte. How to draw a graph. *Proceedings London Mathematical Society*, 13(52):743–768, 1963.
- [22] W. Whiteley. Motion and stresses of projected polyhedra. *Structural Topology*, 7:13–38, 1982.
- [23] H. Whitney. A set of topological invariants for graphs. *Amer. J. Math.*, 55:235–321, 1933.
- [24] F. Zhang. *Matrix Theory*. Springer, 1999.